

Texture Classification based on Complete Magnitude Texton Co-occurrence Matrix using Machine Learning Classifiers

Ujwala Bhoga¹, V Vijaya Kumar²

¹Research Scholar, Department of Computer Science and Engineering,
Anurag University, Hyderabad, India, ujwalacse@anurag.edu.in

²Professor, Dean-School of Engineering, Anurag University, Hyderabad, India,
drvvk144@gmail.com

Across an extensive number of fields dealing with computer vision, including medical imaging and autonomous cars, classifying textures is an important part that plays a crucial role. This paper derived a magnitude relation between textons with three and two identical pixels with non textons on a 2x2 grid. This is named as Complete Magnitude-based Texton (CMT), a novel texture descriptor that aims to improve texture classification performance. The co-occurrence matrix (CM) is derived on the proposed CMT image. The GLCM features on CMT-CM derive characteristics of texture, and changes in magnitude. Various machine learning classifiers are used for classification, and their accuracies are compared. In this study, we assessed how well the CMT-CM descriptor performed on a number of standard datasets, including the Brodatz, MIT-Vistex, UIUC, Outex, STex, and FMD datasets, and we compared its performance with that of cutting-edge approaches. The results of our research clearly demonstrate that the CMT-CM descriptor is capable of achieving a greater degree of accuracy in texture classification tasks when compared to both conventional methods and other advanced descriptors. The findings emphasize, the proposed CMT-CM can enhance texture classification accuracy in different fields. The proposed technique provides a resilient and effective solution for precise and dependable texture analysis, with notable implications for both practical implementations and theoretical investigations in texture categorization.

Keywords: Texture Classification, Feature Extraction, Complete Magnitude based Texton Co-occurrence Matrix.

1. Introduction

The field of computer vision has seen texture analysis rise to prominence in recent years. Texture constitutes a fundamental element in many pattern recognition and computer vision applications, aiding in the classification process by examining the content of image textures. Texture's properties, such as roughness, irregularity, uniformity, and smoothness, are crucial in differentiating various qualities. Texture classification is essential in critical fields such

satellite or aerial imaging analysis [1], industrial inspection [2], biological image analysis [3], face analysis [4] and biometrics [5-6], image compression [7], object recognition [8], and image retrieval based on content [9]. Recognizing and understanding surfaces rely heavily on it.

Feature-extraction and classification are two subproblems that can be taken into consideration while attempting to solve the texture classification problem. The calculation of the attributes that constitute texture is the most significant component of texture classification. This is because texture is a defining characteristic. Although the extraction of robust texture attributes is crucial for the overall efficacy of a texture classification system, most research emphasizes the feature extraction aspect of the process. However, it is still challenging to develop texture characteristics that are resistant to the imaging environment, provide a high level of discrimination and effectiveness, and is computationally efficient. This competence encompasses the ability to endure fluctuations in illumination, rotation, point of view, scale, occlusion, and noise levels. Research that has been conducted in this field on a consistent basis over the course of a number of years has contributed in the development of a considerable number of different theories and algorithms. There is no guarantee that the characteristics that are derived from one classification application are applicable to the other applications in the course of the classification process.

Deriving texture features from grayscale images is a standard practice. The approaches for texture feature extraction are categorized into five distinct types depending on the specific texture components they aim to identify: i) statistical, ii) model, iii) transform, iv) structural [10], and v) learning-based methods. The analysis of the spatial arrangement of grey-level values adjacent to a pixel in an image serves as the basis for the development of statistical approaches. Comprehensive information about the targeted region may be obtained using first-order statistical variables, such as mean, variance, maximum, minimum, and histogram-based representations of grey-level distributions. These properties are invariant to translation and rotation, necessitating reduced computational cost. Matrices such as the grey-level co-occurrence matrix (GLCM) [11] and the grey-level run-length matrix (GLRLM) [12] are used to construct second-order statistical characteristics, which display local grey-level intensity associations. Higher-order statistical features, such as local binary patterns (LBP) [13], emphasize intensity transition patterns within specific sub-regions and exhibit greater resilience to image noise.

During the period 1980-90, methods based on frequency and models were the main focus of texture analysis research. Laws filter-banks [14], fourier transform [15], and wavelets transform [16] were among the frequency-based approaches that were widely used during this time period. Model-based methods, such as fractal models [17] and Markov random fields [18], became more important at the same time. In the early 2000s, statistical descriptor, local binary patterns became potential descriptor for local textures. Subsequently, other versions of local binary patterns were presented. LBP-based algorithms and its modifications have been significant in numerous image processing applications, including feature classification, age classification, recognition of faces, image retrieval based on content, and medical imaging applications. The search for textural characteristics that do not change over time inspired the development of local invariant approaches such as the scale-invariant feature transform [19] and the histogram-of-orientated gradients [20]. Texture analysis strategies have evolved from

early frequency-based and model-based approaches to the present focus on local and invariant texture descriptors. Bag-of-textons [21] and bag-of-words [22] techniques were the first to be used in 2001, marking the beginning of the transition from manual to automated approaches. In these methods, an image dictionary is created, and then, using that dictionary as a basis, images are represented as histograms. Since 2012, deep learning methods garnered momentous attention in research, and their applications have expanded to include texture analysis among other computer vision issues [22-23]. This time represents a turning point in the direction of using deep learning to improve texture analysis results and other computer vision domains even more.

The Local Binary Pattern (LBP) played a major role and influenced many researchers to work beyond and proposed many variants to LBP. The original Local Binary Pattern (LBP) [13] texture descriptor encodes local patterns by comparing neighbourhood pixel values to define a binary code based on whether neighbouring pixels are larger or smaller than the central pixel. Classifying local textures is computationally efficient and effective. LBP is sensitive to noise, lacks scale and rotation invariance, has poor discriminative capacity in complicated scenes, and ignores global spatial information. Moreover, neighbourhood and fixed pattern size matter. Numerous variations of LBPs have been created by the researchers. In order to inhibit the operator's sensitivity to rotation, rotation-invariant (LBPri r,p) [23] was proposed. With the goal of improving the performance of computing and lowering the dimensionality, uniform LBP (LBPu2 r,p) [23] is proposed. To enhance the representation of texture patterns and structures in images, center symmetric-local binary pattern (CS-LBP) [24] was proposed. Another variant, Local Directional Pattern (LDP) [25-26] is designed to capture directional information in local image neighborhoods, making it suitable for textures with distinct directional features. In the recent years the robust LBP variations have been suggested by the scholars. The Multi Direction- Local Binary Pattern (MD-LBP) [27] method captures intricate texture characteristics in several directions, but it also introduces complexity and can be susceptible to noise. Multi-Level Directional Cross Binary Patterns (MLD-CBP) [28] combines several radial and orientation data, improving the acquisition of texture details, nonetheless, it does make the feature space more complicated. Local Triangular Coded Pattern (LTCP) [29] enhances noise resistance by examining triangular pixel correlations, although at the expense of increased implementation intricacy. The Gabor Contrast Patterns (GCP) [30] method integrates Gabor filters with Local Binary Patterns (LBP) to analyze macro and micro textures, however it incurs significant computing expenses. The Neighbourhood influenced Local Binary Pattern (NLBP) [31] improves texture classification accuracy by analyzing correlations between neighboring pixels, declines when applied to scaled images, despite its use of overlapping submatrices to improve LBP. Two Dimensional-Cooccurrence Local Binary Pattern (2D-LCoLBP) [32] efficiently gathers information from several neighborhoods and scales, ensuring scale invariance. However, this approach requires significant computational resources. Directional Magnitude Local Hexadecimal Patterns (DMLHP) [15] method captures both the orientation and magnitude of texture in 16 different directions. However, it has a tendency to overfit the data and may face difficulties in generalizing to new examples. The Directional Binarized Random Features (DBRF) [14] approach provides efficient texture classification by extracting gradients; however it is susceptible to noise and lacks adaptation for complicated datasets. The LBP, LDP and other variants are integrated with GLCM and texton features for an efficient methodology.

Statistical methods are intuitive, straightforward to implement, and somewhat flexible and resilient, while also making the feature space more intricate. The above discussed statistical descriptors offer diverse solutions for texture analysis, providing researchers and practitioners with a rich set of tools for various applications.

2. Literature Review

Textons are essential building blocks for describing basic patterns in a local 2x2 microgrid. For the purpose of representing more complicated patterns, these straightforward patterns capture crucial textural information. Julesz [33–34] introduced the concept of textons, marking a significant advancement in understanding how the human visual system discerns textures. Textons represent fundamental micro-structures within images (and videos), essentially serving as the elemental units of pre-attentive human visual perception. These textons manifest as blobs characterized by color, length, and orientation, taking the form of lines, elongated blobs, and dots [33–35]. For a more in-depth exploration and mathematical models of textons, further details can be found in [36]. A brief survey of texton methods is given as follows: texton cooccurrence matrix (TCM) [37], multi texton histogram (MTH) [38], complete texton matrix (CTM) [39], and the noise resistant fundamental units of complete texton matrix (NRFUCTM) [40] are some examples of works that are closely related to one another in this particular field. The texton cooccurrence matrix (TCM) [37] was initially developed with the purpose of determining the degree of spatial correlation that exists between textons that are contained inside a particular texture image. By utilizing a co-occurrence matrix, it is able to encode information regarding the spatial correlation that exists between textons. Haralick's work on the gray-level cooccurrence matrix (GLCM) served as the source of inspiration for this method. TCM has a focus on the appearance frequency of distinct edges and textons, in contrast to GLCM, which performs calculations to determine the frequency of appearance of different grey levels. An improved version of the TCM, which is referred to as the multi texton histogram (MTH) [38], was proposed by Lie et al. two years after their initial work on the TCM [37]. In contrast to TCM, which was designed to depict texture, MTH has been proposed as a method for representing images that contain a variety of different textures. Because it stores information on the spatial correlation of colours and texture orientations, it possesses the benefits of both the co-occurrence matrix and the colour histogram.

The following drawbacks of TCM and MTH have been identified by this study:

- i) TCM identifies texton patterns that consist solely of three or four identical pixels, disregarding patterns that contain two identical pixels.
- ii) Production of the ultimate texton image via TCM requires an exhausting fusing operation.
- iii) The MTH technique selectively detects a restricted set of texton patterns characterized by two identical pixels.
- iv) In situations where three or more pixels possess an identical intensity level, MTH introduces ambiguity into the process of texton identification. This ambiguity results from the fact that MTH disregards texton patterns consisting of three identical pixels.
- v) Full texton patterns on a 2x2 grid are not precisely defined by either the TCM or MTH methods.
- vi) Texton indexes are not substituted for 2x2 texton microgrids in the majority of texton-based approaches. As a result of deriving only a few or partial texton patterns, these methods have this limitation. In addition, the fusing operation of TCM precludes it from supporting substitution with texton indexes. Figures 1 and

2 depict the TCM and MTH frameworks, correspondingly. The CTM addressed the above issues.

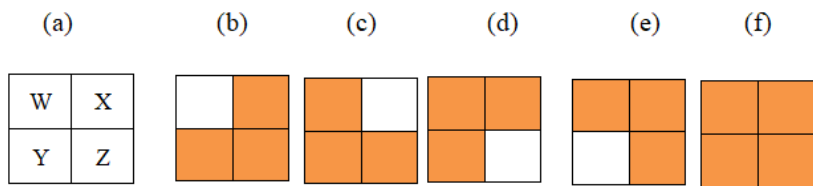


Figure 1: Five Texton types used in TCM (a) 2×2 grid (b) T_1 (c) T_2 (d) T_3 (e) T_4 and (f) T_5



Figure 2: Four Texton types defined in MTH (a) 2×2 grid (b) T_1 (c) T_2 (d) T_3 and (e) T_4

Expanding upon earlier research such as TCM and MTH, Kumari et al. [39] proposed a texton based approach for encoding heterogeneous images. By taking a wider range of textons into consideration than earlier techniques, their approach known as complete texton matrix (CTM) aimed to improve information representation. Eleven textons are included in CTM, as opposed to TCM and MTH with 5 and 4 textons respectively, giving a more thorough depiction. Nevertheless, CTM is limited to textons and does not provide edge or gradient location information. The image is converted to grayscale, divided into non-overlapping 2×2 grids, and each grid is matched with a unique texton as a consequence of the CTM method, producing eleven texton maps. The framework of CTM is shown in figure 3&4 on an image patch of 6×6 . The image is divided into 2×2 micro grids and on each micro grid the CTM indices are computed. The 2×2 grid is replaced with CTM index. In the literature other variations to these basic approaches are proposed.

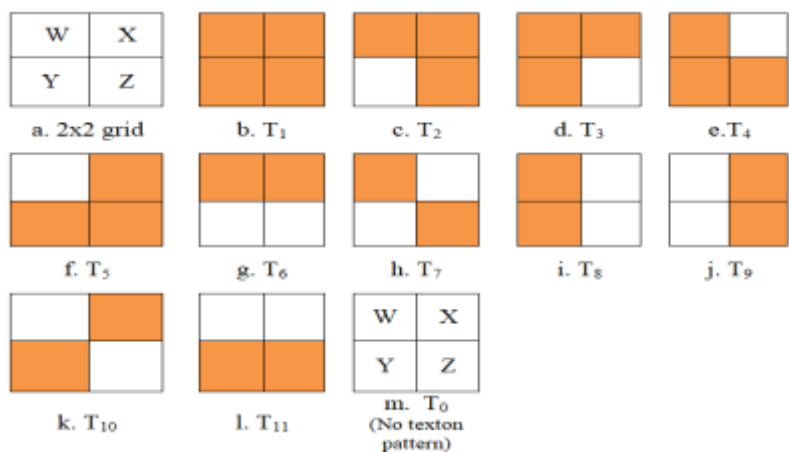


Figure 3: The Texton types defined in CTM: (a) 2×2 grid (b) $T_0 - T_{11}$

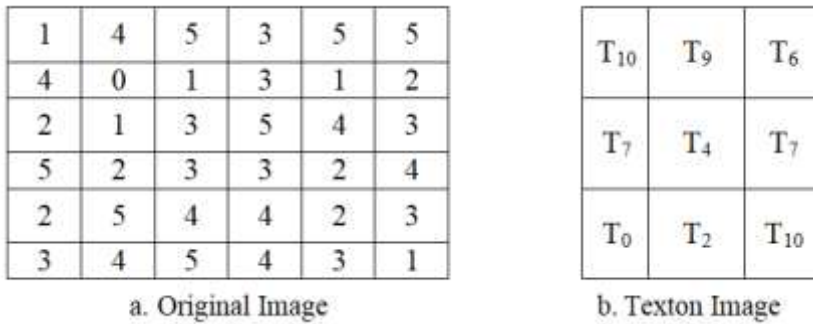


Figure 4: CTM on a 2x2 grid

3. Methodology

The local neighborhood approaches have become the popular approaches for many computer vision applications for the last 30 years. The methods derived on a 2x2 microgrid, textons and motifs [6] have become popular in texture classification, content based image retrieval and the other applications of image processing. The proposed method is based on the textons, and it is an extension to the previous texton methods derived for the texture classification. The existing texton methods TCM [37], MTH [38], CTM [39], FTM [41] and CHFTiCM [42] achieved good results in CBIR and texture classification. These methods derived textons based on the number of pixels exhibiting the same intensities on a 2x2 grid. The research discovered one significant fact that, the earlier texton-based methods didn't derive a relationship between the textons and the non-textons of the 2x2 microgrid. The above fact is addressed in this paper by deriving the magnitude relationship among textons and non-textons of a 2x2 microgrid. The proposed framework of proposed Complete Magnitude based Texton Co-occurrence Matrix (CMT-CM) is shown in figure 5.

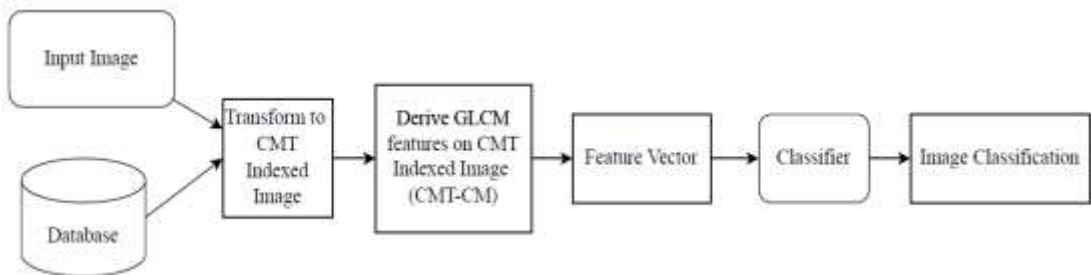


Figure 5: Framework of proposed method CMT-CM

The proposed Complete Magnitude based Texton Co-occurrence Matrix (CMT-CM) initially considered the following textons of two cases: i) textons with two identical pixels as shown in figure 6.a (T_{20} , T_{21} , T_{22} , T_{23} , T_{24} , T_{25}) ii) textons with three identical pixels as shown in figure 6.b. (T_{30} , T_{31} , T_{32} , T_{33}). These textons are denoted as T_{si} where s indicates the number of identical pixels considered and i indicate the texton index with s -type. Further this research established the proposed magnitude relationship between textons and non-textons of the above

two cases.

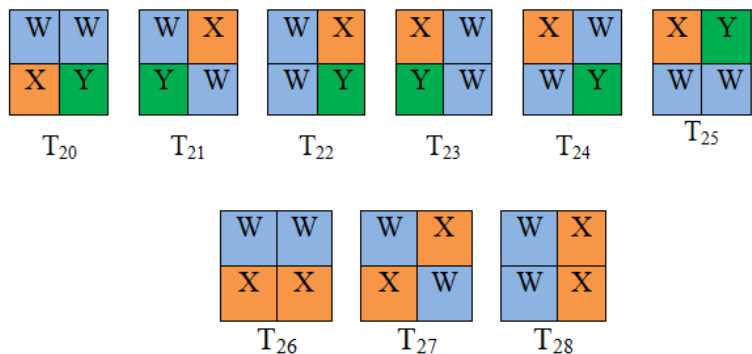


Figure 6.a: Textons with two identical pixels

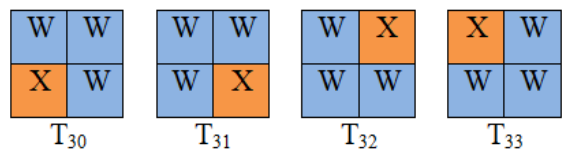


Figure 6.b: Textons with three identical pixels

In the above figures W, X and Y represent three different grey level intensities. The textons with 3-identical pixels of figure 6.b exhibits only two different grey levels W and X on a 2x2 grid, where W and X represents the texton and non-texton pixels respectively. This research derived two magnitude relationships between the grey level values of W and X for each of the textons of figure 6.b.

The magnitude relation between W and X is derived as follows:

Case: H: $W > X$;

Case: L: $W < X$;

Case: E: $W = X$. Not possible with the three identical pixels. In this case, results a texton with square pattern, where all four pixels exhibit the same grey level value.

The case H, L and E represents the grey level values of texton pixels are higher, lower and equal to the non texton pixels respectively.

The above two cases of relationships (H and L) derive two new structural patterns for each of the above texton patterns T₃₀, T₃₁, T₃₂, and T₃₃. The T₃₀ of figure 6.b is split into two different textons by the present research, based on magnitude relation between W and X. These textons are named as Magnitude Texton (MT) with 'H and L' indicating the texton grey level 'W' is high and low respectively with respect to non texton pixel X, (figure 7). In the same way, the textons T₃₁, T₃₂, and T₃₃ are split into MT_{31H}, MT_{32H}, MT_{33H} ($W > X$), and MT_{31L}, MT_{32L}, MT_{33L} ($W < X$) i.e., six textons are derived with different magnitudes by the present research. Thus

the four texton patterns of three identical pixels derive a total of eight MTs as shown in figure 7 and they are indexed from MT_0 to MT_7 .

MT_{30H}	MT_{30L}	MT_{31H}	MT_{31L}	MT_{32H}	MT_{32L}	MT_{33H}	MT_{33L}
C:H:W>X	C:L:W<X	C:H:W>X	C:L:W<X	C:H:W>X	C:L:W<X	C:H:W>X	C:L:W<X
on T_{30}	on T_{30}	on T_{31}	on T_{31}	on T_{32}	on T_{32}	on T_{33}	on T_{33}
MT_0	MT_1	MT_2	MT_3	MT_4	MT_5	MT_6	MT_7

Figure 7: Complete Magnitude Textons (CMT) with three identical pixels

The textons with two identical pixels of figure 6.a exhibits three (T_{20} to T_{25}) and two (T_{26} to T_{28}) different grey levels termed as case1 and case2 respectively. This paper established the magnitude relationship between three identical pixels of figure 6.a as given in case1.

Case 1: When $X \neq Y$ (This case derives interestingly four major magnitude relations between the intensity levels W, X and Y of figure 6.a)

Case: HH: $W > X$ & $W > Y$

Case: HL: $W > X$ & $W < Y$

Case: LH: $W < X$ & $W > Y$

Case: LL: $W < X$ & $W < Y$

The above case1 (when $X \neq Y$) derive new magnitude based structural patterns or magnitude textons (MT) for each of the above texton patterns with two identical pixels T_{20} , T_{21} , T_{22} , T_{23} , T_{24} and T_{25} . For example, texton T_{20} is re-designed by the present research as MT_{20HH} , MT_{20HL} , MT_{20LH} and MT_{20LL} (figure 8). The MT_{20HH} , MT_{20LL} indicates the patterns or textons when $W > X$ & $W > Y$ and $W < X$ & $W < Y$ respectively. The MT_{20HL} , MT_{20LH} indicates the patterns or textons when $W > X$ & $W < Y$ and $W < X$ & $W > Y$ respectively. In the same way, the textons T_{21} , T_{22} , T_{23} , T_{24} and T_{25} lead into MT_{21HH} , MT_{22HH} , MT_{23HH} , MT_{24HH} and MT_{25HH} ($W > X$ & $W > Y$), MT_{21HL} , MT_{22HL} , MT_{23HL} , MT_{24HL} and MT_{25HL} ($W > X$ & $W < Y$), MT_{21LH} , MT_{22LH} , MT_{23LH} , MT_{24LH} and MT_{25LH} ($W < X$ & $W > Y$), and MT_{21LL} , MT_{22LL} , MT_{23LL} , MT_{24LL} and MT_{25LL} ($W < X$ & $W < Y$) respectively. That is the present research derives four different magnitude based textons (MT) on each of the textons from T_{20} to T_{25} . Thus the six textons with magnitude relation derives the 24 micro textons by the present research and they are indexed from MT_8 to MT_{31} .

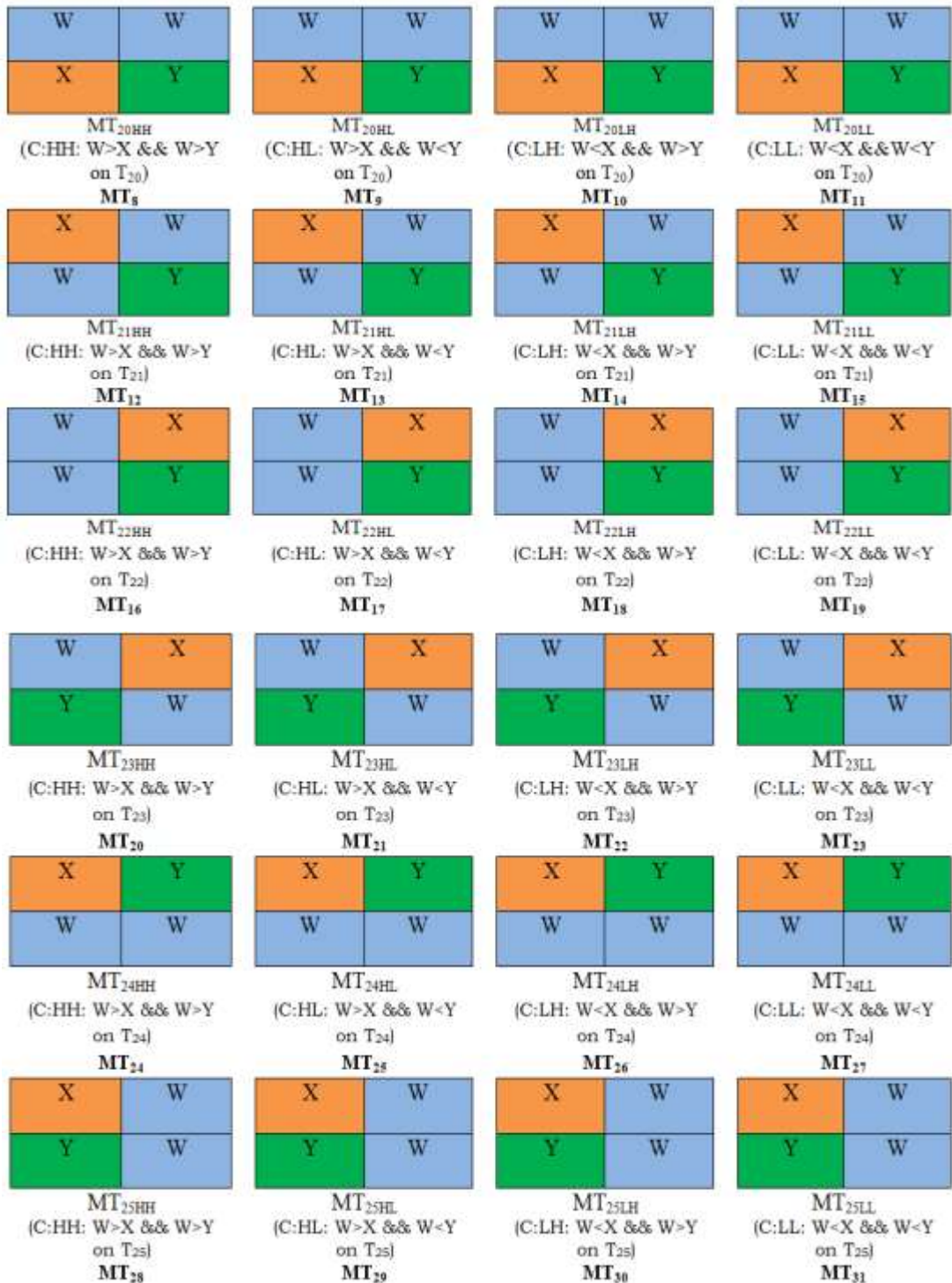


Figure 8: Complete Magnitude Textons (CMT) with two identical pixels when X!=Y

The textons T_{26} to T_{28} derives multiples of two identical pixels ($W \neq X$) shown in Figure 6.a. The case 2 compares the magnitude relations between intensity values of W and X and thus it derives two sub cases.

Case 2:

Case H: $W > X$

Case L: $W < X$

Thus this research derived six different MTs for T_{26} , T_{27} and T_{28} i.e., each of the texton pattern derives two MTs and these are indexed from MT_{32} to MT_{37} .

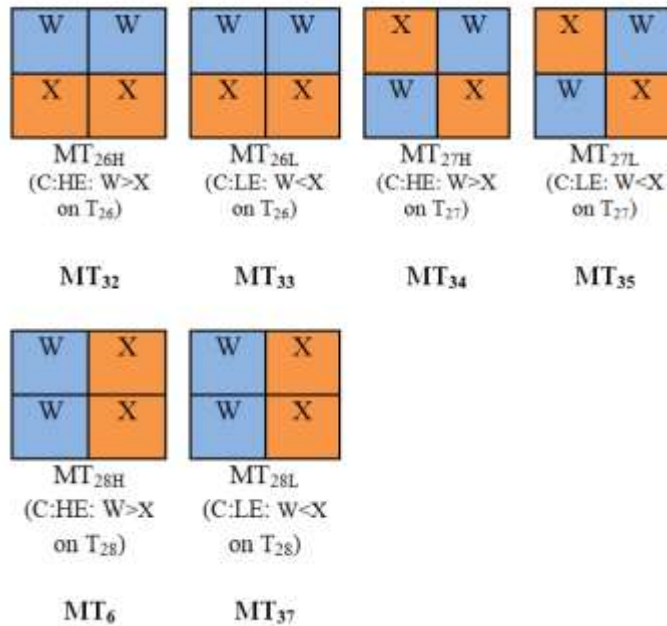


Figure 9: The Magnitude Textons for the textons with two identical pixels (case2)

The combinations of textons from figure 7 to figure 10 are named as Complete Magnitude Textons (CMT) by the present paper. Thus the textons with three grey levels derived eight magnitude based textons (MT) namely MT_0 to MT_7 , the textons with two identical pixels with case 1 derives 24 MTs represented from MT_8 to MT_{31} and the same with case2 derives 6 MTs denoted from MT_{32} to MT_{37} . Further this research considered the texton with all identical pixel and no identical pixels as shown below and represented them as MT_{38} and MT_{39} .

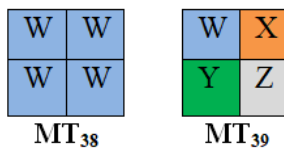


Figure 10: The Magnitude Textons for the textons with four identical pixels and zero

identical pixels

The MT_{38} texton does not derive any magnitude relation since all four pixels of 2×2 grid exhibit the same grey level. The MT_{39} does not form any texton thus the magnitude relation is not derived i.e. the magnitude relationship is derived between the texton patterns and non texton patterns. Thus the present research derived a total of 40 magnitude textons (MT_0 to MT_{39}).

This paper derived co-occurrence matrix (CM) on CMT and named this as CMT-CM. The GLCM features derived on CMT-CM are homogeneity, contrast, entropy, correlation, and inverse difference moment.

4. Database Description:

To illustrate the efficacy of the proposed Complete Magnitude based Texton Co-occurrence Matrix (CMT-CM) descriptor, comprehensive research is conducted on six prominent texture databases, namely the Colored Brodatz Texture (CBT), MIT-VisTex, Outex, University of Illinois Urbana-Champaign (UIUC), Salzburg Texture (Stex), and Flickr Material Database (FMD). The example pictures from these datasets are presented in figures 11, 12, 13, 14, 15, and 16, respectively.

The well-known CBT texture dataset includes natural texture photos captured in studio lightening. It consists of 112 texture image classes. Transforming the Brodatz texture database into a color version is what the CBT database is all about.

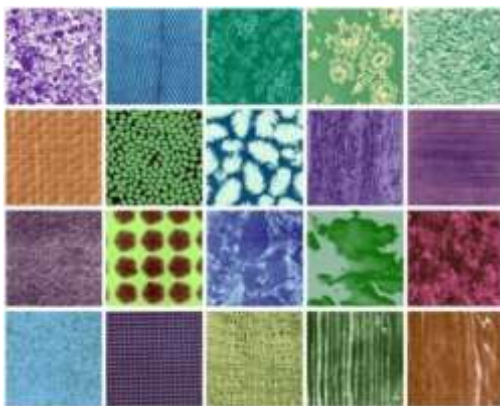


Figure 11: Sample Colored Brodatz Textures

The MIT-VisTex dataset was developed by the MIT Media Laboratory. Images created using VisTex, in contrast to Brodatz, look more natural because they were not created in a lab. It comprises 167 colorful reference textured pictures, each measuring 786 by 512 pixels, contingent of the scene's orientation (other sizes are also available).



Figure 12: Sample VisTex Textures

The Outex dataset is the most extensive dataset about texture categories. The collection comprises 320 categories of texture photos, each captured under 3 lighting circumstances and 9 rotation angles, devoid of perspective and size variations. The two expanded Outex datasets (Outex TC00010 and Outex TC00012) are extensively utilized in texture classification to evaluate the rotation and illumination invariance of texture characteristics.



Figure 13: Sample Outex-TC-00010c Textures

The Salzburg Texture database (Stex) has a substantial collection of 476 color texture images obtained from Salzburg, Austria. STex is offered in three distinct packages: i) stex-1024.zip comprises 476 color pictures, each with dimensions of 1024x1024 pixels. ii) stex-512.zip comprises 476 color pictures, each measuring 512x512 pixels, which have been downsampled from 1024x1024 images. iii) stex-512-split. The 512x512 photos were divided into 16 non-overlapping tiles to create the 7616 color, 128x128 images that are included in the zip file. Our research utilized the stex-512 split dataset. Sample Stex texture pictures are depicted in figure 14.



Figure 14: Sample STex Textures

The University of Illinois Urbana-Champaign (UIUC) collection has 25 texture classes, each containing 40 uncalibrated, unregistered pictures with dimensions of 640x480. It has less severe lighting fluctuations than CURET, but it still exhibits considerable perspective and scale changes along with non-rigid deformations. Sample textures from UIUC are depicted in figure 15.

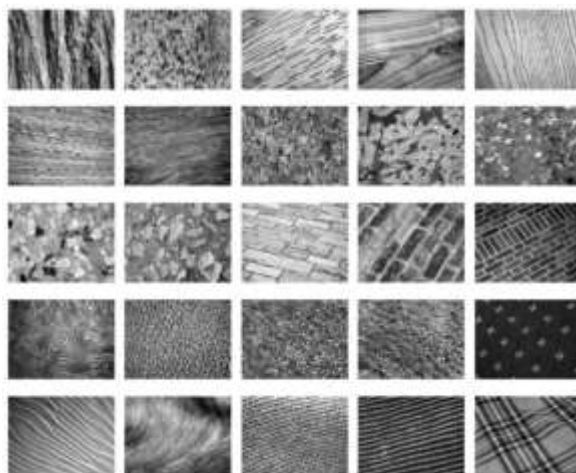


Figure 15: Sample UIUC Textures

The Flickr Material Database (FMD) comprises color photographs of surfaces categorized into 10 common material types: foliage, fabric, leather, glass, paper, metal, stone, plastic, water, and wood. Every category has 100 photos, comprising 50 close-ups and 50 standard views, with dimensions of 512x384 pixels. Each image features surfaces from a singular material category in the foreground and was meticulously chosen from over 50 possibilities to guarantee a diversity of illumination situations, compositions, colors, textures, surface forms, material sub-types, and item connections. Figure 16 presents some textures of FMD.



Figure 16: Sample Flickr Material Database Textures

Table 1 Database summary for images

S.No.	Database	True Image Size	Image Size Considered	Classes Taken into Account	Class-wise Images	Overall image count
1	CBT	640X640	128X128	112	25	2800
2	VisTex	51X512	128X128	40	16	640
3	Outex- TC10	128X128	128X128	24	180	4320
4	Stex	128X128	128X128	476	16	7616
5	UIUC	640X480	640X480	25	40	1000
6	FMD	512X384	512X384	10	100	1000

5. Results and Discussions:

The study conducted extensive research on texture analysis to assess the effectiveness of the proposed descriptor “Complete Magnitude based Texton Co-occurrence Matrix (CMT-CM)”. For each of the databases listed, this study used the proposed CMT-CM descriptor to calculate the GLCM features: homogeneity, contrast, entropy, correlation, and inverse difference moment and derived feature vector for each database mentioned. In order to evaluate the performance of the proposed CMT-CM descriptor, the feature vectors of the databases were fed into the five different classifiers: Support Vector Machine (SVM), K-nearest neighbours (KNN), Decision Tree (DT), Random Forest (RF) and Naive Bayes (NB).

This paper initially converted the image into a CMT image with index values ranging from 0 to 39. The second step involves deriving the matrix of co-occurrences from the CMT, which transforms the CMT image into CMT-CM. The above mentioned GLCM features are derived on CMT-CM. These features are fed to above five machine learning classifiers. The classification accuracies obtained with the proposed CMT-CM descriptor for the above mentioned classifiers are shown in the table 2 and figure 17.

Table 2 Classification Accuracies obtained with the proposed CMT-CM descriptor for different classifiers on various databases

Database	Naive Bayes (NB)	Decision Tree (DT)	Random Forest (RF)	K-nearest neighbors (KNN)	Support Vector Machine (SVM)
Colored Brodatz Texture (CBT)	85.37	90.58	92.65	87.42	96.47
MIT Vision Texture (Vistex)	87.44	88.76	90.84	84.68	94.63
Outex TC-00010	87.53	85.36	88.62	91.21	95.37
Salzburg Texture (Stex)	82.69	87.62	92.13	86.58	93.65
University of Illinois Urbana-Champaign (UIUC)	84.53	91.47	90.74	92.31	92.58

Flickr Material Database (FMD)	74.65	77.24	81.35	75.93	83.79
Average	83.70	88.64	89.39	86.36	92.75

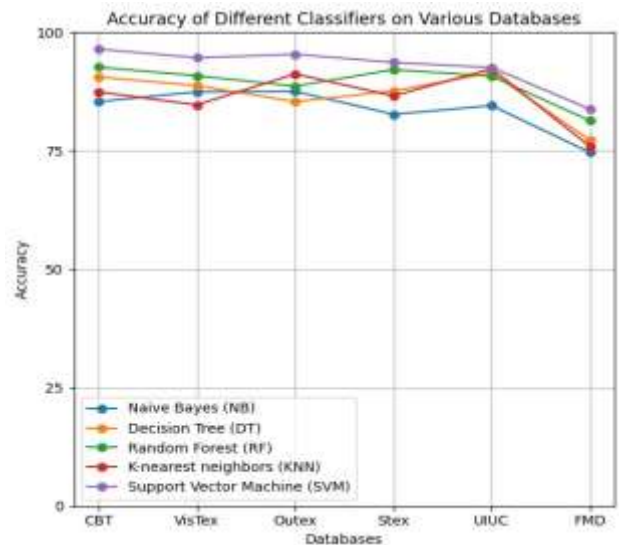


Figure 17: Classification accuracies obtained with the proposed CMT-CM descriptor for different classifiers

This paper conducted experiments on the datasets given in table 1. The proposed CMT-CM method has given high accuracy on Brodatz followed by Outex TC-00010, Vistex, Stex, UIUC and FMD datasets. The improved accuracy in classifying the Brodatz dataset can be due to its well-defined and high-quality texture patterns, which offer obvious and identifiable characteristics for analysis. By providing a dataset with a wide range of textures that are well regulated, classifiers are able to generalize more efficiently, resulting in improved performance. Moreover, having a large number of training examples for each class greatly facilitates the development of a strong and resilient model.

Support Vector Machine classifier has achieved high classification rate followed random forest, decision tree, k-nearest neighbours and naive bayes using the proposed CMT-CM method. Support Vector Machines excel at achieving high accuracy on texture databases because they can optimize the margin between classes, efficiently handle high-dimensional spaces, and leverage the kernel technique to manage non-linear interactions. Support Vector Machines have regularization settings that stop them from overfitting and set decision limits based only on the support vectors. This makes them resistant to noise. The precisely formulated convex optimization problem guarantees convergence to the global optimum, and their flexibility with varied kernel functions enables them to adjust to diverse datasets. The properties of Support Vector Machines make them highly successful for difficult texture classification problems that involve a large number of dimensions. As a result, SVMs outperform other classifiers in terms of performance. The classification accuracy of the proposed CMT-CM descriptor is compared with other existing methods and these are shown in table 3 and figure 18.

Table 3 Classification accuracies of proposed method and different texture descriptors on various databases

State-of-art-methods and Proposed method	Databases					
	Colored Brodatz Texture (CBT)	MIT Vision Texture (Vistex)	Outex TC-00010	Salzburg Texture (Stex)	University of Illinois Urbana-Champaign (UIUC)	Flickr Material Database (FMD)
Local Directional pattern (LDP) [35] [2010]	90.52	91.35	91.58	89.74	86.43	72.6
Local Directional Gradient Pattern (LDGP) [9] [2017]	92.73	87.33	91.24	90.64	88.67	77.68
Complete Texton Matrix (CTM) [27] [2017]	91.56	69.93	92.46	90.21	91.18	65.46
Directional Magnitude Local Hexadecimal Patterns (DMLHP) [12] [2021]	88.25	93.25	89.64	84.53	82.86	76.19
Gabor Contrast Patterns (GCP) [39] [2023]	92.65	94.38	91.63	86.64	84.15	78.62
Neighbourhood influenced Local Binary Pattern (NLBP) [40] [2023]	87.77	82.19	86.74	85.57	81.3	76.19
Proposed method CMT-CM	96.47	94.63	95.37	93.65	92.58	83.79

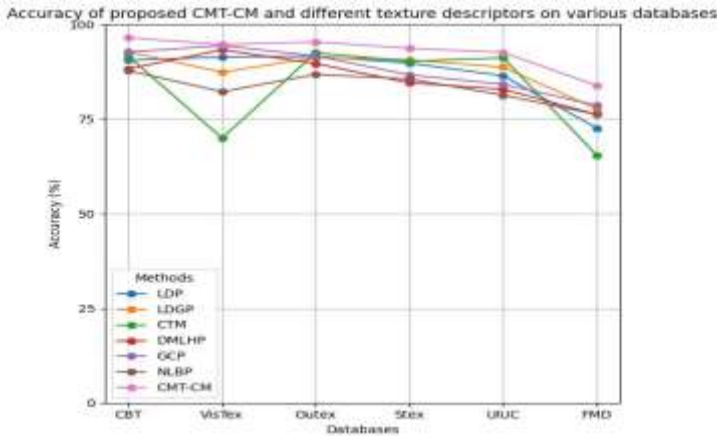


Figure 18: Classification accuracies of proposed CMT-CM and different texture descriptors on various databases

This paper compared the classification results of the proposed descriptor CMT-CM with the existing local neighborhood descriptors, Local Directional Pattern (LDP), Local Directional Gradient Pattern (LDGP), Directional Magnitude Local Hexadecimal Patterns (DMLHP), Gabor Contrast Patterns (GCP), and Neighbourhood influenced Local Binary Pattern (NLBP), as well as the texton-based method Complete Texton Matrix (CTM).

The Local Directional Pattern (LDP) improves upon the Local Binary Pattern (LBP) by encoding edge responses in eight directions using Kirsch masks, making it more robust to noise and illumination changes. While LDP offers better accuracy and robustness, it has the

drawbacks: i) doesn't consider the center pixel; ii) finding the K value is difficult; iii) increases computational complexity and storage requirements due to the directional edge response calculations. The Local Directional Gradient Pattern (LDGP) enhances face recognition by encoding pixel relationships in four directions, reducing feature length and computational complexity. While it offers good accuracy and noise robustness, it has the disadvantages: i) reliance on gradient calculations can be computationally expensive, especially for large-scale applications; ii) struggle with textures that lack clear directional patterns; iii) sensitive to noise and illumination variations. The Directional Magnitude Local Hexadecimal Patterns (DMLHP) analyzes texture orientation and magnitude in 16 directions to provide a complete feature collection. Although it excels in texture classification, it suffers from several disadvantages. i) may struggle with color, shape, or semantics; ii) computationally intensive; iii) overfits various datasets; iv) unsuitable for large-scale or real-time applications; v) limits generalization across different image categories. The Gabor Contrast Patterns (GCP) combines Gabor filters and Local Binary Patterns (LBP) to capture both macro- and micro-texture features, resulting in a robust texture descriptor. While it excels in texture classification with high discriminative power, it has the disadvantages: i) higher computational cost and complexity; ii) limited validation across diverse datasets. The Neighbourhood influenced Local Binary Pattern (NLBP) enhances traditional LBP by analyzing correlations between neighboring pixels using overlapping submatrices of various sizes (3x3, 5x5, 7x7) and applying statistical thresholding methods like mean, mode, median, and max to extract more precise texture features. NLBP demonstrated improved accuracy and robustness, particularly in noisy conditions. However, It has the disadvantages: i) struggle to capture local information at a microgrid level in larger submatrices (5x5, 7x7); ii) accuracy drops slightly with scaled images.

The proposed method (CMT-CM) consistently ranks at or near the top in accuracy across a variety of texture and material classification datasets, demonstrating outstanding performance, after comparison with the above-listed methods in the table 3. It exhibits versatility and robustness by achieving maximum accuracies of 92.58% and 83.79% on the UIUC and FMD datasets, respectively. In comparison to other algorithms, CMT-CM outperforms Gabor Contrast Patterns (GCP), which also performs well but trails on UIUC and FMD datasets with 84.15% and 78.62%, respectively. This is due to similarity of textures in different classes of images in UIUC and lot of textural variations in the images of same class in the FMD dataset. The Complete Texton Matrix (CTM) method performs well on the Outex TC-00010 (92.46%) and Stex (90.21%) datasets, but it fails to meet expectations on the FMD dataset (65.46%) due to textural variations in the images of same class in the FMD dataset. The CMT-CM has achieved better accuracy on FMD dataset. The Directional Magnitude Local Hexadecimal Patterns (DMLHP) has shown competitive results (93.25%) on VisTex dataset, but proposed method has outperformed on all the datasets. Local Directional Gradient Pattern (LDGP) and Neighbourhood influenced Local Binary Pattern (NLBP) both demonstrate acceptable accuracy results; however, the proposed method CMT-CM consistently outperforms both of these methods.

All things considered, the proposed method CMT-CM seems to be a very successful strategy, constantly attaining better results on a variety of datasets, demonstrating its resilience and ability to generalize in texture and material classification tasks. The proposed method CMT-

CM achieved a superior classification rate as a result of the following operations.

The research contributions are:

1. Derivation of all conceivable textons with two and three identical pixels with magnitude relations thus deriving a new direction over the existing methods on textons.
2. More local information can be obtained significantly by deriving all likely textons on a 2x2 grid by taking into account the magnitude relationship between the pixels that make up and do not make up a texton.
3. There is a reduction in the overall size of the CM as a result of replacing the 2 x 2 grid with MT indexes, which makes it possible to interface with other frameworks when it is required.

The proposed framework possesses significant value due to its thorough experimental research on six natural databases and its systematic and comprehensive comparison of classification findings with current descriptors.

6. Conclusion

The proposed research introduces the CMT-CM, a novel feature descriptor that enhances texture classification by capturing spatial relationships and texture variations in images. By establishing relationships between texton and non-texton elements in a 2x2 grid and generating GLCM features, the CMT-CM effectively differentiates various texture classes. The evaluation using several classifiers, particularly the SVM, highlights its ability to handle high-dimensional feature spaces efficiently, especially when sample sizes are relatively small compared to feature complexity. The results demonstrate that CMT-CM consistently achieves high accuracy across multiple datasets, underscoring its robustness and versatility. The findings emphasize the proposed CMT-CM can enhance texture classification accuracy in different fields. Its simplicity in feature extraction and computational efficiency make it a practical and powerful tool for texture recognition tasks, suggesting significant potential for broad applications in texture-based datasets. The proposed technique provides a resilient and effective solution for precise and dependable texture analysis, with notable implications for both practical implementations and theoretical investigations in texture categorization.

References

1. J. He, H. Ji, and X. Yang, "Rotation invariant texture descriptor using local shearlet-based energy histograms," *IEEE Signal Process. Lett.*, vol. 20, no. 9, pp. 905–908, Sep. 2013.
2. X. Xie and M. Mirmehdi, "TEXEMS: Texture exemplars for defect detection on random textured surfaces," *IEEE Trans. Pattern Anal. Mach. Intell.*, vol. 29, no. 8, pp. 1454–1464, Aug. 2007.
3. L. Nanni, A. Lumini, and S. Brahmam, "Local binary patterns variants as texture descriptors for medical image analysis," *Artificial Intelligence in Medicine*, vol. 49, pp. 117–125, Feb. 2010.
4. D. Huang, C. Shan, M. Ardabilian, et al., "Local binary patterns and its application to facial image analysis: a survey," *IEEE Trans. Syst. Man Cybern. C: Applications and Reviews*, vol. 41, no.6, pp. 765–781, Nov. 2011.

5. G. Zhao and M. Pietikainen, "Dynamic texture recognition using local binary patterns with an application to facial expressions," *IEEE Trans. Pattern Anal. Mach. Intell.*, vol. 29, no. 6, pp. 915–928, Jun. 2007.
6. N. Jhanwar, S. Chaudhuri, G. Seetharamanc, and B. Zavidovique, "Content based image retrieval using motif co-occurrence matrix," *Image and Vision Computing*, vol. 22, no.14, pp.1211–1220. Dec. 2004.
7. L. Gatys, A. S. Ecker, and M. Bethge, "Texture synthesis using convolutional neural networks," in *Proc. Adv. Neural Inf. Process. Syst.*, pp. 262–270, 2015.
8. J. Zhang, M. Marszałek, S. Lazebnik, and C. Schmid, "Local features and kernels for classification of texture and object categories: A comprehensive study," *Int. J. Comput Vision*, vol. 73, no. 2, pp. 213–238, Jun. 2007.
9. J. Sivic and A. Zisserman, "Video Google: A text retrieval approach to object matching in videos," in *IEEE Int. Conf. Comput. Vis.*, pp. 1470–1477, Oct. 2003.
10. Laleh Armi and Shervan Fekri-Ershad "Texture Image Analysis and Texture Classification Methods - A Review," *International Online Journal of Image Processing and Pattern Recognition* vol. 2, no.1, pp. 1-29, Jan. 2019.
11. R. M. Haralick, K. Shanmugam, and I. Dinstein, "Textural features for image classification," *IEEE Transactions on Systems, Man, and Cybernetics*, vol. SMC-3, no. 6, pp. 610–621, Nov. 1973.
12. R. M. Haralick, "Statistical and structural approaches to texture," *Proceedings of the IEEE*, vol. 67, no. 5, pp. 786–804, May.1979.
13. T. Ojala, M. Pietikäinen, and T. Mäenpää, "Multiresolution gray-scale and rotation invariant texture classification with local binary patterns," *IEEE Trans. Pattern Anal. Mach. Intell.* vol. 24, no. 7, Jul. 2002.
14. Xiaochao Zhao , Fang Xu , Yi Ma, Zhen Liu , Min Deng, Umer Sadiq Khan, and Zenggang Xiong "Dynamic Texture Classification Using Directional Binarized Random Features," *IEEE Access*, vol.11, May 2023.
15. Ayesha Khan, Ali Javed , and Muhammad Tariq Mahmood et. al, "Directional Magnitude Local Hexadecimal Patterns: A Novel Texture Feature Descriptor for Content-Based Image Retrieval," *IEEE Access*, vol. 9, Sep. 2021.
16. Y. Ma, "Number Local binary pattern: An Extended Local Binary Pattern,"2011 International Conference on Wavelet Analysis and Pattern Recognition, pp. 272-275, Sep. 2011.
17. A. P. Pentland, "Fractal-based description of natural scenes," *IEEE Trans. Pattern Anal. Mach. Intell.*, vol. PAMI-6, no. 6, pp. 661–674, Nov. 1984.
18. F. S. Cohen, Z. Fan, and M. A. Patel, "Classification of rotated and scaled textured images using Gaussian Markov random field models," *IEEE Trans. Pattern Anal. Mach. Intell.*, vol. 13, no. 2, pp. 192–202, Feb. 1991.
19. D. G. Lowe, "Distinctive image features from scale-invariant keypoints," *Int. J. Comput. Vis.*, vol. 60, no. 2, pp. 91–110, Jan. 2004.
20. N. Dalal and B. Triggs, "Histograms of oriented gradients for human detection," in *Proc. IEEE Comput. Soc. Conf. Comput. Vis. Pattern Recognit.*, pp. 886–893, Jul. 2005.
21. T. Leung and J. Malik, "Representing and recognizing the visual appearance of materials using three-dimensional textons," *Int. J. Comp. Vision.*, vol. 43, no. 1, pp. 29–44, Jun. 2001.
22. S. Chakraborty, SK.Singh, and P. Chakraborty, "Local directional gradient pattern: a local descriptor for face recognition," *Multimedia Tools and Applications*, vol.76, no.1, pp.1201–1216, Nov. 2015.
23. T. Ojala, M. Pietikäinen, and T. Mäenpää, "Multiresolution gray-scale and rotation invariant texture classification with local binary patterns," *IEEE Trans. Pattern Anal. Mach. Intell.*, vol. 24, no. 7, pp. 971–987, Jul. 2002.
24. Marko Heikkilä, Matti Pietikäinen, and Cordelia Schmid, "Description of Interest Regions

- with Center-Symmetric Local Binary Patterns,” *ICVGIP 2006*, LNCS 4338, pp. 58–69, 2006.
25. B. Zhang, Y. Gao, S. Zhao and J. Liu, “Local derivative pattern versus local binary pattern: face recognition with high-order local pattern descriptor,” *IEEE Trans. on Image Processing*, vol. 19, no. 2, pp. 533-544, Feb. 2010.
26. T. Jabid, M. H. Kabir and O. Chae, “Local Directional Pattern (LDP) for face recognition,” *2010 Digest of Technical Papers International Conference on Consumer Electronics (ICCE)*, pp. 329-330, Feb. 2010.
27. J. Liu, Y. Chen and S. Sun, “A novel local texture feature extraction method called multi-direction local binary pattern,” *Multimed Tools Appl*, vol. 78, pp.18735–18750, Feb.2019.
28. M. Kas , I. El khadiri , Y. El merabet, Y. Ruichek , and R. Messoussi , “Multi Level Directional Cross Binary Patterns: New handcrafted descriptor for SVM-based texture classification,” *Engineering Applications of Artificial Intelligence*, vol. 94, 103743, Sep.2020.
29. R. Arya & E. R. Vimina, “Local Triangular Coded Pattern: A Texture Descriptor for Image Classification,” *IETE Journal of Research*, vo. 69, no.6, pp. 3267–3278, May. 2021.
30. Abdul Wahab Muzaffar, Farhan Riaz et. al, “Gabor Contrast Patterns: A Novel Framework to Extract Features from Texture Images,” *IEEE Access*, vol. 11, pp. 60324-60334, May, 2023.
31. Akash Dev V and A. Baskar, “NLBP - An Improved Local Binary Pattern for Texture Classification using Correlational Features of Neighbouring Pixels,” *2023 Innovations in Power and Advanced Computing Technologies (i-PACT)*, pp. 1-7, 2023. doi: 10.1109/i-PACT58649.2023.10434916.
32. Xiuli Bi , Yuan Yuan, Bin Xiao , Weisheng Li, and Xinbo Gao, “2D-LCoLBP: A Learning Two-Dimensional Co-Occurrence Local Binary Pattern for Image Recognition,” *IEEE Transactions on Image Processing*, vol. 30, pp. 7228-7240, Aug. 2021
33. B. Julesz, “Textons, the elements of texture perception, and their interactions,” *Nature* 290, pp. 91-97 , Mar. 1981.
34. B. Julesz, “A theory of preattentive texture discrimination based on first-order statistics of textons,” *Biological Cybern*, vol.41, no.2, pp.131–138, Aug. 1981.
35. B. Julesz, JR. Bergen, “Human Factors and Behavioral Science: Textons, The Fundamental Elements in Preattentive Vision and Perception of Textures,” *Readings in computer vision*, pp. 243–256, 1987.
36. Zhu, SC., Guo, Ce., Wang, Y. et.al, “What are textons?,” *Int. J. Comput Vision*, vol. 62 , pp.121–143, Apr. 2005.
37. Guang-Hai Liu, Jing-Yu Yang, “Image retrieval based on the texton co-occurrence matrix,” *Pattern Recog* , vol.41, no.12, pp.3521–3527, Dec. 2008.
38. Guang Hai Liu, Lei Zhang, Ying-Kun Hou, Zuo-Yong Li, and Jing-Yu Yang, “Image retrieval based on multi-texton histogram,” *Pattern Recogn*, vol. 43, no.7, pp. 2380–2389, Jul. 2010.
39. Y.Sowjanya Kumari, V. Vijaya Kumar, and Ch. Satyanarayana, “Texture classification using complete texton matrix,” *Int. J. of Image Graphics Signal Processing* vol.9, no.10, pp.60-68, Oct. 2017.
40. Y.Sowjanya Kumari, V. Vijaya Kumar, and Ch. Satyanarayana, “Classification of textures based on noise resistant fundamental units of complete texton matrix,” *Int. J. Image Graphics Signal Process*, vol.10, no.2, pp. 43-51, Feb.2018.
41. G. Bindu Madhavi, V. Vijaya Kumar, and K. Sasidhar, “Image Retrieval Based On Color and Full Texton Matrix Histogram (C&Ftmh) Features,” *International Journal of Innovative Technology and Exploring Engineering (IJITEE)*, vol. 8, no.8, pp. 507-521, Jun. 2019.
42. G. Bindu Madhavi, V. Vijaya Kumar, and K. Sasidhar, “Content Based Image Retrieval using Color and Full Texton Index Co-occurrence Matrix (FTiCM) Features,” *International Journal of Recent Technology and Engineering (IJRTE)*, vol.8, no.1, pp. 2277-3878, May. 2019.